Experimental Results for the Rheological and Rheo-Optical Behavior of Poly(ethylene terephthalate)/ Liquid-Crystalline Polymer Blends

M. T. Cidade,[1] A. R. Menon,[2] C. R. Leal,[3,4] C. K. S. Pillai[2]

[1]*Materials Science Department and CENIMAT, New University of Lisbon, Campus da Caparica, 2829-516 Caparica, Portugal*
[2]*Polymer Division, Regional Research Laboratory (CSIR), Thiruvananthapuram 695019, India*
[3]*ISEL, Polytechnical Institut of Lisbon, Scientific Area of Physics, Rua Conselheiro Emídio Navarro 1, 1949-014 Lisboa, Portugal*
[4]*CFMC, Lisbon University, Avenida Professor Gama Pinto 2, P-1649-003 Lisboa, Portugal*

Received 6 March 2007; accepted 1 August 2007
DOI 10.1002/app.27155
Published online 9 October 2007 in Wiley InterScience (www.interscience.wiley.com).

ABSTRACT: The use of thermoplastic/liquid-crystalline polymer (LCP) blends is recognized as a good strategy for reducing viscosity and improving mechanical properties relative to pure thermoplastics. This improvement, however, is only noticeable if the LCP fibrillates, *in situ*, during processing and the fibrils are kept in the solid state. In this article, we report a morphological, rheological, and rheo-optics study performed with two blends of poly(ethylene terephthalate) with a LCP, Rodrun LC3000 (10 and 25 wt % LCP content), and we show that the obtained droplet-shape relaxation time (the time the deformed droplet took to regain its spherical form after the cessation of flow) allowed for the explanation of the morphological observations. In fact, the droplet-shape relaxation time was higher for the blend with higher LCP content, for the higher experimentally accessible shear rates, and still increased at the highest shear rate, which explained the fibrils of the LCP dispersed phase observed in this blend, whereas for the lower LCP content blend, the droplet-shape relaxation time reached a low-value plateau for higher shear rates, which explained the absence of fibrillation in this blend. © 2007 Wiley Periodicals, Inc. J Appl Polym Sci 107: 1280–1287, 2008

Key words: blends; liquid-crystalline polymers (LCP); morphology; rheology; thermoplastics

INTRODUCTION

Liquid-crystalline polymers (LCPs) are materials that present exceptional mechanical properties; however, due to their high cost, they have limited applications. On the other hand, common thermoplastics are relatively inexpensive polymers even though their mechanical strength is much lower than those of LCPs. Allying the properties of the two kinds of polymers seems to be a good strategy for obtaining materials with improved mechanical properties at a reasonable cost. Motivated by this interesting combination, blends of these two kinds of materials have been the subject of intense research in the last 2 decades.[1–13]

The mechanical improvement and easier processability obtained for these blends are, however, dependent on the *in situ* fibrillation of the LCP dispersed phase during processing, which is due to the immiscibility of both components and the tendency of the LCP to orient with the flow.[14]

While studying the influence of the LCP content in the morphological and mechanical properties of poly(ethylene terephthalate) (PET)/Rodrun LC3000 blends, we concluded that the morphology, as studied by scanning electron microscopy (SEM), of a blend with 10 wt % LCP content (hereafter referred to as 90PET/10LCP) did not present any fibrils, contrary to what happened with a blend with a higher content of LCP (25 wt %, hereafter referred to as 75PET/25LCP). To determine the explanation for these findings, we characterized the rheological and rheo-optical behaviors of these two blends.

The study of droplet deformation in sheared emulsions is a complex subject. Taylor[15,16] investigated, for the first time, the droplet deformation and breakup under slow shear flow of an isolated Newtonian droplet immersed in an immiscible Newtonian fluid. Some experimental and theoretical analyses were performed in the following decades and summarized in several reviews.[17,18] In these studies, it was found that an isolated droplet immersed in an immiscible fluid is spherical at rest; however, when a

Correspondence to: M. T. Cidade (mtc@fct.unl.pt).
Contract grant sponsors: GRICES, Science and Technology Foundation, Portugal, DST, India (under a bilateral cooperation project).

shear field is imposed on the emulsion, a competition between interfacial tension effects, which tend to keep the droplet spherical, and shear, which tends to deform it, appears. The extent of droplet deformation depends on which of these two phenomena is predominant. An increase in shear stress (induced deformation) leads to an increase in droplet deformation, and when the interfacial tension no longer balances the shear stress, the droplet breaks up. These effects are accounted for by two dimensionless numbers, the capillary number ($Ca = \eta_m R_0 \dot{\gamma}/\sigma$, where $\eta_m, R_0, \dot{\gamma},$ and σ, are the matrix viscosity, the undeformed droplet radius, the shear rate, and the interfacial tension, respectively) and the viscosity ratio ($\lambda = \eta_d/\eta_m$, where η_d is the viscosity of the dispersed phase). When the capillary number exceeds a certain critical value (which is a function of the viscosity ratio), droplet breakup occurs.

Another phenomena observed in concentrated sheared emulsions is coalescence, which results from the collision of two droplets and gives rise to a bigger droplet. Coalescence may be the only phenomena present when one deals with low capillary numbers and in processes where the shear rate is suddenly decreased or even suppressed, such as in relaxation processes.

Until the 1990s, only isolated, nonconfined (drop radius/gap width $\ll$ 1) Newtonian droplets, dispersed in Newtonian fluids, observed in the velocity gradient direction, were studied. In recent years, there has been a great development in the field of deforming droplets in immiscible fluids. Guido et al.[19,20] introduced a method that allows observation of sheared droplets in two perpendicular directions; along the velocity gradient direction (top view) and along the vorticity axis of shear flow (side view), which allows for three-dimensional observations of the droplets. The extension of the two Newtonian components to an emulsion composed of an isolated Newtonian droplet dispersed in a viscoelastic fluid (Boger fluid) was performed by Guido et al.,[21] and an isolated viscoelastic droplet immersed in a Newtonian fluid was studied by Sibillo et al.[22] The influence of confinement on the steady-state microstructures of emulsions sheared between parallel plates in a regime where the average droplet dimension is comparable to the gap width between the confining walls was studied by Pathak et al.[23] and Vananroye et al.,[24] among others.

To our knowledge, a system composed of two viscoelastic fluids under high deformations in confined regimes has never been investigated in detail, and it was not our intention to do so in this study. Our only purpose was to find an expedited method that would allow us to explain the different microstructures observed in our two PET/Rodrun LC 3000 blends.

EXPERIMENTAL

Materials

PET (Reliance Industries, Mumbai, India) and Rodrun LC3000 (Unitika, Japan) were used to produce LCP/thermoplastic blends. The thermoplastic used for the preparation of the blends was a commercial polymer with an intrinsic viscosity of 0.8 dL/g. The LCP was an aleatory copolyester of 60 mol % *p*-hydroxybenzoic acid and 40 mol % PET. The melting temperatures of the matrix and dispersed phase as determined by differential scanning calorimetry (DSC 92, Setaram, Lyon, France) at a heating rate of 3°C/min were 257 and 189°C, respectively.

The zero-shear viscosity of PET was about 30 Pa s at 260°C, and Rodrun LC 3000 did not present any zero-shear viscosity for the lower experimentally accessible shear rate, which means that it was not possible to determine the viscosity ratio for this blend. However, for the lower shear rate proved, the viscosity ratio was about 0.15, which showed that the viscosity ratio must have been lower than unity.

Processing

PET was processed in a single-screw extruder (described later), and the blends were prepared in two steps; in the first one, the two polymers were mixed in a Rheocord mixer (Thermo-Haake, Karlsruhe, Germany) at 260°C, and in the second step, the mixture was processed in a single-screw extruder (Rheomex 252P, Karlsruhe, Germany) with a die temperature of 260°C. The screw had a length/diameter ratio of 25 and a compression ratio of 3. The screw rotation speed was 20 rpm for PET and 25 rpm for the blends. The die of the extruder was a sheet and ribbon die with a diameter of 25 mm.

Two contents of LCP, 10 and 25 wt %, were used for the blends. Before processing, the materials were dried in an oven for 24 h at 90°C.

Morphological characterization

The morphological characterization was performed by SEM with a Zeiss DSM 962 scanning electron microscope (Oberkochen, Germany). All of the cryogenically fractured samples were previously coated with a Polaron SC502 (Fisons Instruments, Rodanio, Italy) and then examined by SEM at an accelerating voltage of 10 kV. These observations were performed for cryogenically longitudinal and transversal cuts of the final extrudates.

Rheological characterization

The rheological behavior of the PET/Rodrun LC3000 blends was studied for the pure components and for the two blends.

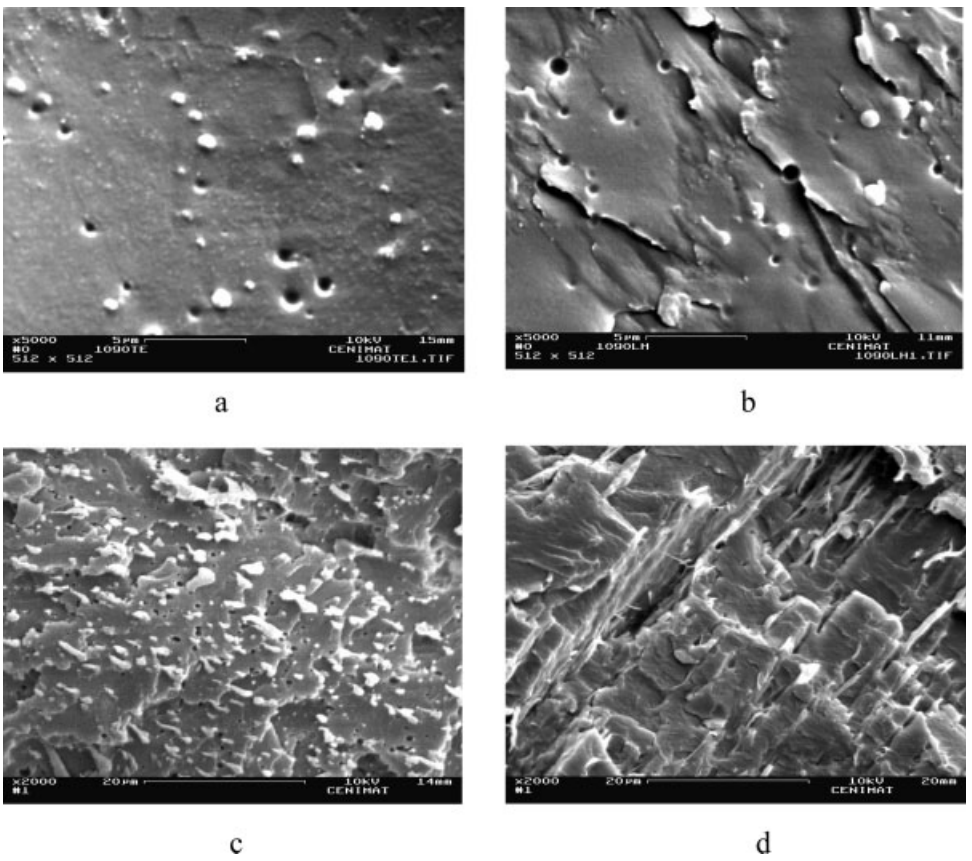

Figure 1 SEM microphotographs of 90PET/10LCP (a) transversally fractured and (b) longitudinally fractured (magnification 5000×) and 75PET/25LCP (c) transversally fractured and (d) longitudinally fractured (magnification, 2000×).

All of the samples were premolded into disclike shapes with diameters of 25 mm and thicknesses of 1 mm at 260°C subject to the application of a 5-ton pressure in a heated press from SPEAC (London, UK).

The experiments were carried out in an AR500N stress-controlled rotational rheometer from TA Instruments. All of the measurements were obtained with a cone-and-plate geometry, with a diameter of 25 mm, an angle of 2°, and a gap of 58 μm at 260°C.

The flow curve for the shear viscosity as a function of the shear rate under steady-state conditions was obtained with the following procedure: preshear of shear rate $\approx$ 10 s^{-1} for 300 s, followed by an equilibration of 300 s, and followed by a step shear stress increment procedure, ranging from 10 to 15000 Pa (for PET and the blends) and from 1 to 1000 Pa (for pure LCP).

The oscillatory experiments, used to characterize the elastic modulus and loss modulus as a function of the angular frequency, were carried out by the application of a strain of 10% at an angular frequency range between 0.06283 and 251.3 rad/s.

Rheo-optical characterization

Optical observation of the blends under shear was performed with a Linkam CSS 450 shearing system. The blends were premolded in discs of appropriate diameter and thickness before they were onto the two parallel glass plates used as geometry.

To observe the dispersed phase (LCP), the samples were heated to 280°C and then cooled back to 260°C, the measuring temperature, and the gap was set to 50 μm, which created a confined environment (droplet size to gap ratio of 0.28 and 0.36 for the two blends). Thermal equilibration was allowed for 10 min more.

We conducted microscopic observations under cross-polarized light, by placing the cell on an optical microscopy stage (Olympus BX40 microscope, Middlesex, UK). The observations were performed along the velocity gradient direction (top view). The images were analyzed with image analysis software (PCTVision (Braunschweig, Germany)).

RESULTS AND DISCUSSION

Morphology

To study the morphology of the two blends (90PET/10LCP and 75PET/25LCP), SEM was performed for the extrudates. In addition to the typical transversal cuts, longitudinal cryogenic fracture was performed to better clarify whether there was formation of LCP fibrils.

Figure 1 presents the SEM microphotographs obtained. Figure 1 shows that, in fact, the existence of fibrils was easier to observe in samples that were longitudinally fractured [cf. Figure 1(c,d)] as expected, but more important than this, it shows that for the lower LCP content blend (90PET/10LCP), no fibrillation occurred [Fig. 1(b)]. On the other hand, for the higher LCP blend (75PET/25LCP), fibrillation occurred, which is clearly shown in Figure 1(d), where the LCP fibrils were dispersed in the PET matrix.

Rheological characterization

The influence of LCP addition to a thermoplastic polymer in the rheological behavior of thermoplastic/LCP blends has been widely studied,[8,25–29] and in general, it has been observed that the increase of LCP content leads to a decrease in the viscosity and complex modulus when viscosity ratios are smaller than unity, as was the case in the blends examined in this study.

The flow curve of pure components and blends is presented in Figure 2. The LCP presented a three-region flow curve, which started with a slow shear-thinning region for low shear rates, was followed by a Newtonian plateau at intermediate shear rates, and finished with a stronger shear-thinning region for high shear rates, the common three-region flow curve for LCPs. As shown in Figure 2, the LCP presented the smallest viscosity values in the entire shear-rate range when compared with the PET and the PET/LCP blends.

On the contrary, the thermoplastic matrix, PET, presented a flow curve with the highest viscosity values in the same shear-rate range, starting with a Newtonian plateau, followed by a shear-thinning region for high shear rates, which is common behavior for thermoplastics.

The 90PET/10LCP and 75PET/25LCP blends presented viscosity values between those of the pure components. The increase in LCP content in the blends led to an increase in the internal friction and,

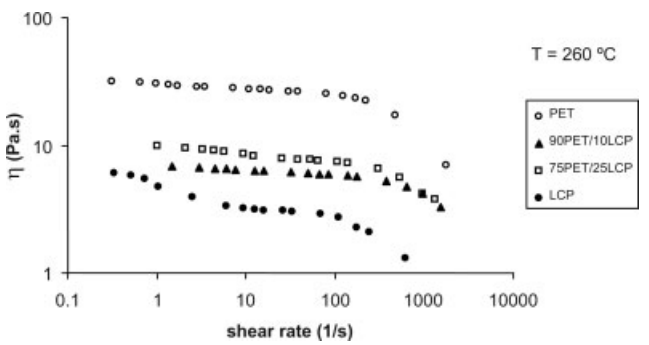

Figure 2 Flow curves for the 90PET/10LCP and 75PET/25LCP blends and for the pure components at 260°C.

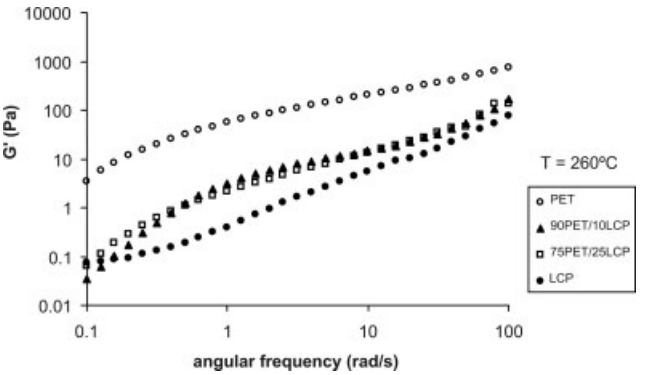

Figure 3 Evolution of the storage modulus (G') with the angular frequency for blends 90PET/10LCP and 75PET/25LCP and for the pure components at 260°C.

consequently, to an increase in the shear viscosity at low and intermediate shear rates in the Newtonian plateau region. For high shear rates, the opposite effect occurred, which led to a crossover between the two curves. This crossover was attributed to the fact that for the lower shear rates, the orientation of the LCP was restricted by the matrix, whereas for higher shear rates, the matrix itself was oriented by the flow, and the orientation of the LCP was now free to occur. This behavior has also been reported in other works with similar blends.[26,27,30]

In the oscillatory shear measurements performed in the linear regime, we found that the pure thermoplastic was the material with the higher elastic modulus, whereas the LCP had the lowest one. The same results were observed for the loss modulus, as shown in Figures 3 and 4.

For the 90PET/10LCP and 75PET/25LCP blends, a similar behavior to the steady-state results was observed but only in the elastic modulus dependence. For low angular frequencies, the 75PET/25LCP blend showed a higher elastic modulus, which was inverted at about 0.8 rad/s, where the 90PET/10LCP blend curve started to present higher elastic modu-

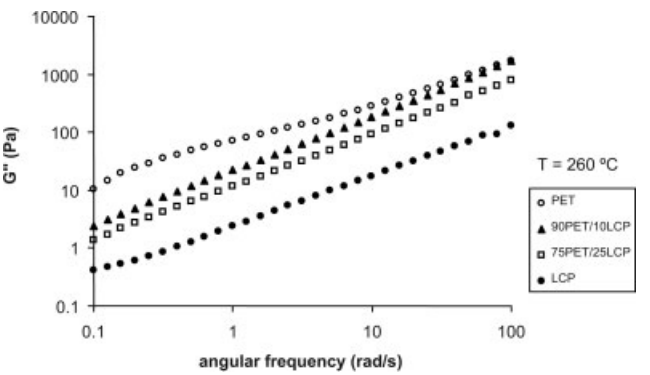

Figure 4 Evolution of the loss modulus (G'') with the angular frequency for the 90PET/10LCP and 75PET/25LCP blends and for the pure components at 260°C.

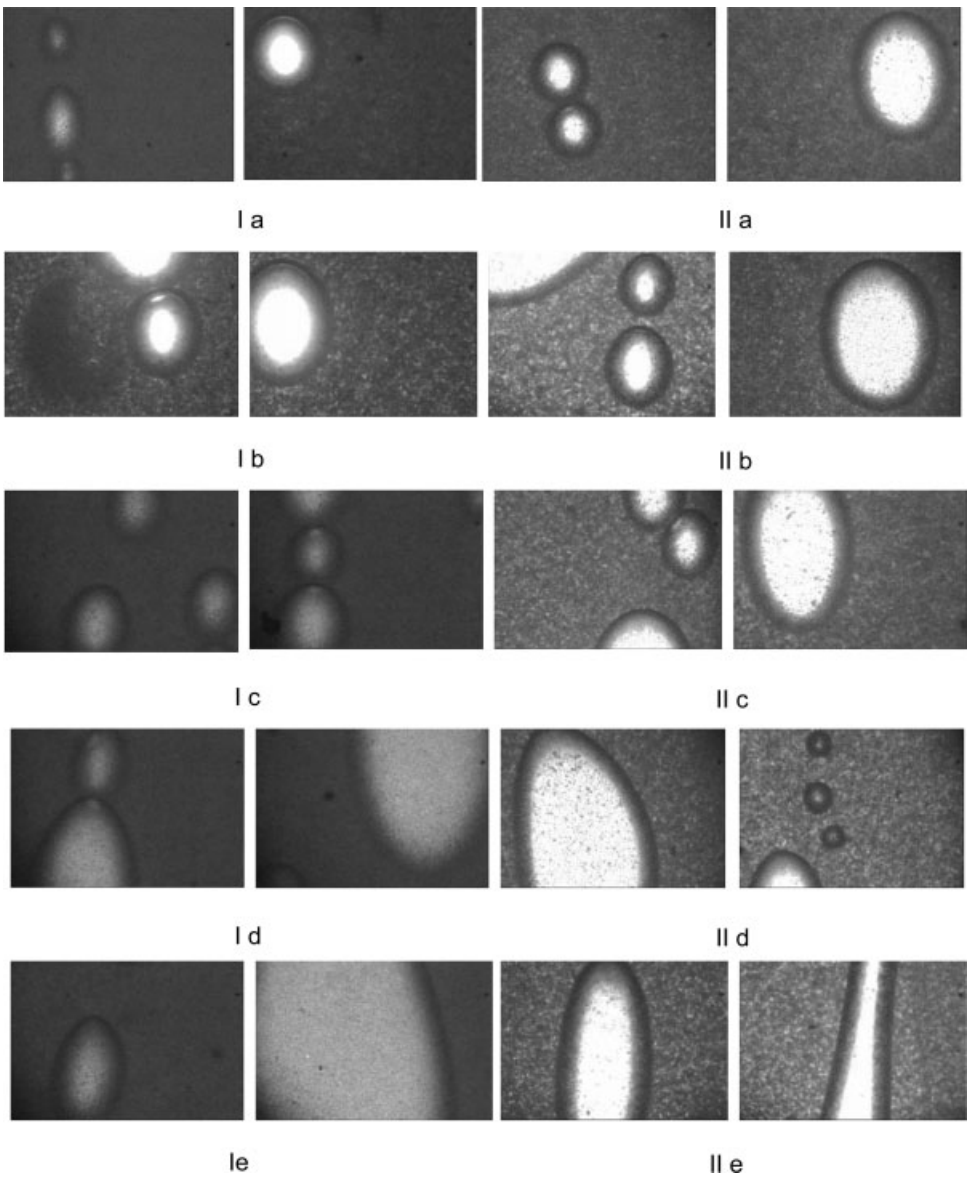

Figure 5 Example of the evolution of the droplet size and deformation with the shear rate for (I) 90PET/10LCP and (II) 75PET/25LCP: (a) 10, (b) 20, (c) 30, (d) 40, and (e) 50 s^{-1} (magnification, 220×).

lus values. For high angular frequencies, both elastic moduli showed basically the same value.

Rheo-optical characterization

Samples of the 90PET/10LCP and 75PET/25LCP blends were observed under shear for shear rates ranging from 5 to 50 s^{-1} and after the cessation of shear. The same sample was used for observations under different shear rates, starting with the lower shear rate and then increasing the shear rate by steps until the higher shear rate was reached. The increase in the shear rate was only performed after the relaxation of the sample subject to the previous shear rate, which led to the coalescence phenomena.

During the observations, photos were taken and videos were recorded after the evolution of different droplets in the same sample. The procedure was repeated for at least four different samples of the same blend, which allowed us to determine the mean values to characterize the droplet evolution as a function of the applied shear rate and after the cessation of shear.

Figure 5 shows an example of the evolution of the droplet size and deformation with shear rate for the lower and higher LCP content blends, 90PET/10LCP and 75PET/25LCP, respectively.

Observations of the photos presented in Figure 5, along with other similar photos not presented here, led us to conclude that both blends presented a big

dispersion of droplet sizes, that no big differences were found for the droplet sizes of both samples (for the same shear rate), and that an increase in the droplet size and deformation extent, as measured by the ratio between the longest and the shortest axis sizes, was observed with increasing shear rate.

In addition, Figure 5 shows that no breakup occurred, which means that the critical capillary number was not exceeded. This conclusion may be explained by the fact that in confined droplets and with viscosity ratios lower than unity, which was our case, breakup of individual droplets can be suppressed, as reported by Vananroye et al.,[31] for a model system of two transparent Newtonian polymers, polydimethylsiloxane (PDMS) dispersed in polyisobutylene (PIB). On the contrary, coalescence phenomena were present, which was anticipated because of the relaxation that took place between the two consecutive shear rates applied, which was responsible for the increase in droplet size with increasing shear rate.

Figure 5 also shows that the droplets organized themselves in only one layer, even for the smaller droplets (low shear rates), where the ratio of droplet size to gap spacing was 0.28 and 0.36 for 90PET/10LCP and 75PET/25LCP, respectively. A critical ratio of 0.5 was determined by Pathak et al.[23] for concentrated blends (up to 35 wt % of the dispersed phase) of the model system PDMS dispersed in PIB to be the value for which the transition from two layers to one layer, due to confinement, occurred. However, Vananroye et al.[24] found, for a dilute blend (up to 10 wt % of the dispersed phase) of PIB dispersed in PDMS, that a single layer was still observed for $2R_0/d \sim 0.25$ (where d is the gap spacing).

Finally, Figure 5 also shows that as long as the droplets were still small enough to observe more than one droplet at the same time, a tendency for the droplets to organize themselves into the so-called pearl necklace structure was observed. This structure was also observed by Pathak et al.[23] and Vananroye et al.[24]

Figure 6 shows the average longest and shortest axis sizes of the deformed droplet, L and D, respectively, as a function of the shear rate. Note that L and B (or r_{max} and r_{min}) usually denote the longest and shortest axis sizes of the droplet (as determined with lateral view observations).[20,24] In our case, L was the projection of the longest axis (usually denoted L_p); however, because it is known that the angle between the longest axis and the direction of flow was a decreasing function of the shear rate (or capillary number; e.g., 20), we expected that our angle was very small because we were dealing with high shear rates, which meant that the projection of the longest axis size had to be similar to the longest axis size itself. Also, D had to be the same as B because we considered the droplet to be ellipsoidal.

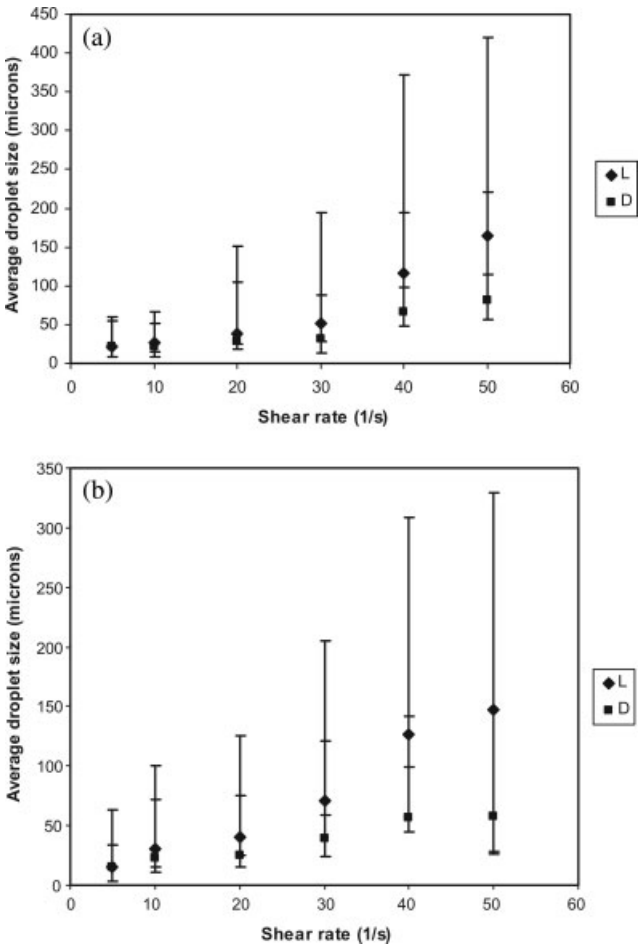

Figure 6 Average droplet size (L and D) as a function of the shear rate for (a) 90PET/10LCP and (b) 75PET/25LCP (the bars represent the maximum and minimum values, not the standard deviation).

As shown in Figure 6, we confirmed some of the findings referred to previously, namely, that the droplet size increased with shear rate, that no significant differences were found for the droplet size of the two samples, and that a big dispersion in droplet size was present in both samples.

The average droplet deformation extent, as measured by the ratio L/D, as a function of shear rate is presented in Figure 7.

From the analysis of Figure 7, we concluded that the average droplet deformation extent increased linearly with the shear rate, with the 75PET/25LCP blend being the one that was more affected by the shear rate; in other words, for this sample, L/D versus the shear rate presented a higher slope.

After the cessation of shear, time was allowed for the relaxation of the droplets until they retracted back to their initial spherical shape. The average relaxed droplet size as a function of shear rate is

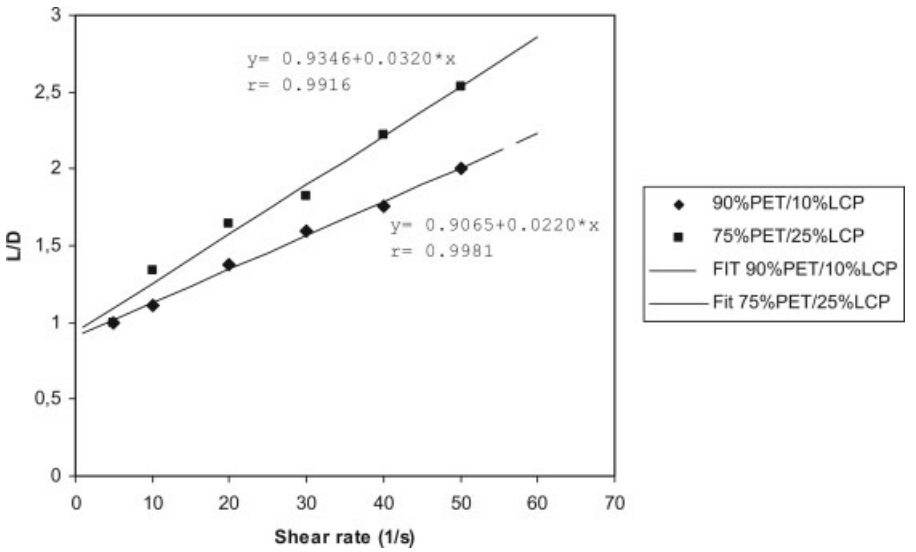

Figure 7 Average droplet deformation extent as a function of the shear rate for 90PET/10LCP and 75PET/25LCP.

presented in Figure 8, where we can see that it also increased linearly with shear rate, with a higher slope for the 75PET/25LCP blend.

By measuring the time elapsed from the moment of cessation of shear to the moment where the complete relaxation of the droplet was achieved, which was determined by the measurement of L/D as a function of time, we calculated the droplet-shape relaxation time as a function of prior shear rate. These results are presented in Figure 9.

The analysis of Figure 9 shows that a significant difference was found for the two blends. For the blend with the lower LCP content, the relaxation times were small and tended to a plateau for the higher shear rates, whereas for the blend with the higher LCP content, the relaxation times were much higher for the higher shear rates and were still increasing at a shear rate of 50 s^{-1}. These results were in accordance with the morphological characterization, which showed that only the 75PET/25LCP blend presented fibrils in the solid state. These results explain why the 10PET/90LCP blend did not present any fibrillation in the solid state. They show that the fibrils may have formed during processing, but after exiting the die, the LCP relaxed faster than it solidified. The fact that the blend was confined between the two surfaces in the rheo-optic device may have caused the relaxation to be slower than when the blend exited the die, which means that the time for the complete relaxation of the droplets may be even lower than the one determined in this study for each blend.

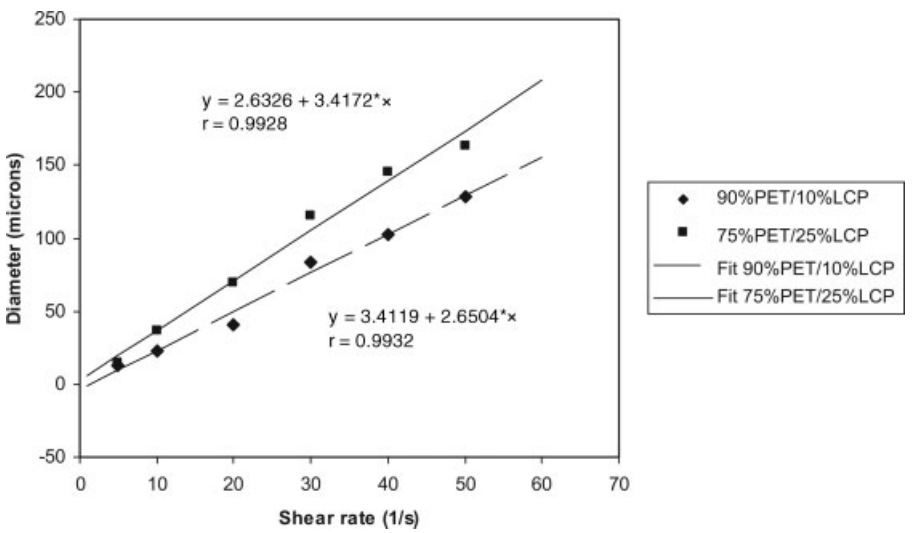

Figure 8 Average relaxed droplet size as a function of the shear rate for 90PET/10LCP and 75PET/25LCP.

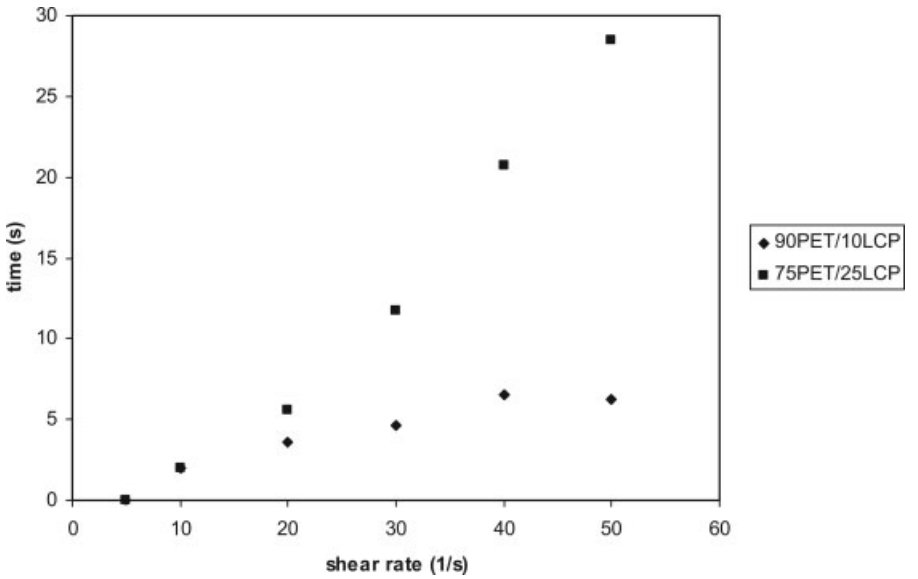

Figure 9 Droplet relaxation time as a function of the prior shear rate for 90PET/10LCP and 75PET/25LCP.

CONCLUSIONS

SEM images of blends of PET with Rodrun LC 3000 with 10 and 25 wt % LCP (90PET/10LPC and 75PET/10LCP, respectively) showed that the smaller LCP content blend did not present fibrils, whereas the blend with the higher LCP content did.

With the preliminary results presented for the rheo-optic observations, we concluded that the existence, or not, of fibrils in the extrudates seemed to be linked to the droplet-shape relaxation time. If the relaxation time was very small, the fibrils had time to relax at the die exit before the molten blend solidified, and the LCP appeared as a dispersion of droplets of irregular size in the PET matrix. On the contrary, if the droplet-shape relaxation time was high enough, the fibrils were frozen along with the molten blend.

References

1. Bhattacharya, S. K.; Tendolkar, A.; Misra, A. Mol Cryst Liq Cryst 1987, 153, 501.
2. La Mantia, F. P.; Valenza, A.; Paci, M.; Magagnini, P. L. J Appl Polym Sci 1989, 38, 583.
3. Ko, C. U.; Wilkes, G. L. J Appl Polym Sci 1989, 37, 3063.
4. Kulichikhin, V. G.; Vasil'Eva, O. V.; Litvinov, I. A.; Antipov, E. M.; Parsamyan, I. L.; Platé, N. A. J Appl Polym Sci 1991, 42, 363.
5. Turek, D. E.; Simon, G. P.; Tiu, C.; Tiek-Siang, O.; Kosior, E. Polymer 1992, 33, 4322.
6. Qin, Y.; Brydon, D. L.; Mather, R. R.; Wardman, R. H. Polymer 1993, 34, 1196.
7. Qin, Y.; Brydon, D. L.; Mather, R. R.; Wardman, R. H. Polymer 1993, 34, 3597.
8. Heino, M. T.; Hietaoja, P. T.; Vainio, T. P.; Seppälä, J. V. J Appl Polym Sci 1994, 51, 250.
9. Wei, K. H.; Kiss, G. Polym Eng Sci 1996, 36, 713.
10. O'Donnel, H. T.; Baird, D. G. Int Polym Process 1996, 11, 257.
11. Wang, H. M.; Yi, X. S.; Hinrichsen, G. Polym J 1997, 29, 881.
12. Tan, L. P.; Yue, C. Y.; Tam, K. C.; Lam, Y. C.; Hu, X. J Appl Polym Sci 2002, 84, 568.
13. Saengsuwan, O.; Bualek-Limcharoen, S.; Mitchell, G. R.; Olley, R. H. Polymer 2003, 44, 3407.
14. Roetting, O.; Hinrichsen, G. J Thermoplast Mater 1997, 10, 524.
15. Taylor, G. I. Proc R Soc London A 1932, 138, 41.
16. Taylor, G. I. Proc R Soc London A 1934, 146, 501.
17. Rallison, J. M. Annu Rev Fluid Mech 1984, 16, 45.
18. Stone, H. A. Annu Rev Fluid Mech 1994, 26, 65.
19. Guido, S.; Villone, M. J Rheol 1998, 42, 395.
20. Guido, S.; Greco, F. Rheol Acta 2001, 40, 176.
21. Guido, S.; Simeone, M.; Greco, F. Polymer 2003, 44, 467.
22. Sibillo, V.; Guido, S.; Greco, F.; Maffettone, P. L. Macromol Symp 2005, 228, 31.
23. Pathak, J. A.; Davis, M. C.; Hudson, S. D.; Migler, K. B. J Colloid Interface Sci 2002, 255, 391.
24. Vananroye, A.; Van Puyvelde, P.; Moldenaers, P. Langmuir 2006, 22, 2273.
25. Viswanathan, R.; Isayev, A. J Appl Polym Sci 1995, 55, 1117.
26. Choi, G. D.; Jo, W. H.; Kim, H. G. J Appl Polym Sci 1996, 59, 443.
27. Choi, G. D.; Kim, S. H.; Jo, W. H. Polym J 1996, 28, 527.
28. Wanno, B.; Samran, J.; Bualek-Limcharoen, S. Rheol Acta 2000, 39, 311.
29. Filipe, S.; Cidade, M. T.; Wilhelm, M.; Maia, J. M. Polymer 2004, 45, 2367.
30. Filipe, S.; Maia, J. M.; Leal, C. R.; Cidade, M. T. J Polym Eng 2005, 25, 527.
31. Vananroye, A.; Van Puyvelde, P.; Moldenaers, P. Langmuir 2006, 22, 3972.